Numerical Investigation on Two-dimensionality in the Traveling Liquidus-zone Method

Satoshi Adachi[1], Yasuyuki Ogata[1], Satoshi Matsumoto[1], Naokiyo Koshikawa[2], Masahiro Takayanagi[1], Shin-ichi Yoda[3] and Kyoichi Kinoshita[1]

Abstract

In order to investigate the two-dimensionality in the traveling liquidus-zone (TLZ) method, the two-dimensional TLZ model is introduced. Basing on the two-dimensional model, the two-dimensionality is defined. From the numerical results in various sample diameters, the two-dimensionality is obtained. In the case of the sample diameter of 2 mm, the two-dimensionality is negligibly small on the ground. However, in the case of 10 mm, the two-dimensionality is large even though under no gravity condition if an InGaAs seed is used.

Introduction

The traveling liquidus-zone (TLZ) method[1, 2] is one of the most advancing growth techniques to obtain a homogeneous crystal of a ternary compound semiconductor such as InGaAs crystals. The feature of the TLZ method is to determine the proper sample translation rate easily for homogeneous crystal growth. In order to determine the translation rate, the one-dimensional theoretical model[3] has been introduced. This model predicts the growth rate precisely. Thus single crystals of 2 mm in diameter and of more than 20 mm in length have been successfully obtained with good reproducibility on the ground. However, it becomes difficult to grow a homogeneous crystal with a larger diameter than 2 mm on the ground. In order to understand the reason for the difficulty, we introduce a two-dimensional TLZ model. By considering the two-dimensional model, definition of two-dimensionality is discussed. To calculate the two-dimensionality, two-dimensional numerical simulations in various sample diameters are carried out. From the numerical results, the two-dimensionality is estimated and is discussed.

Two-dimensional TLZ model

In order to investigate two-dimensionality, a two-dimensional TLZ model is introduced. The generalized expression of solution growth can be described as

$$(C_L - C_S)\, u \cdot \hat{n} = -D \left.\frac{\partial C_L}{\partial n}\right|_{z=int}, \tag{1}$$

where n is a normal direction to an interface, u a vector of growth rate and $\hat{n}$ a unit vector being perpendicular to the interface. Here, we assume that the z-coordinate is a function of the r-coordinate and time t, that is,

$$z = f(r, t). \tag{2}$$

[1] SS Science Project Office, Institute of Space and Astronautical Science, Japan Aerospace Exploration Agency, 2-1-1 Sengen, Tsukuba, 305-8505, Japan

[2] Centrifuge Project Team, Office of Space Flight and Operations, Japan Aerospace Exploration Agency, 2-1-1 Sengen, Tsukuba, 305-8505, Japan

[3] Department of Space Biology and Microgravity Sciences, Institute of Space and Astronautical Science, Japan Aerospace Exploration Agency, 2-1-1 Sengen, Tsukuba, 305-8505, Japan

By using Eq. (2), the unit vector $\hat{n}$ can be described as

$$\hat{n} = \frac{1}{\sqrt{1+\left(\frac{\partial f}{\partial r}\right)^2}}\left(-\frac{\partial f}{\partial r}, 1\right). \tag{3}$$

By substituting Eq. (3) to Eq. (1), the following equation

$$(C_L - C_S)\frac{\partial f}{\partial t} = -D\left(\frac{\partial C_L}{\partial z} - \frac{\partial C_L}{\partial r}\frac{\partial f}{\partial r}\right) \tag{4}$$

is obtained. Here,

$$\left.\frac{\partial C_L}{\partial z}\right|_{z=int} = \left.\frac{\partial C_L}{\partial T}\right|_{z=int}\left.\frac{\partial T}{\partial z}\right|_{z=int} \quad \text{, and} \tag{5}$$

$$\left.\frac{\partial C_L}{\partial r}\right|_{z=int} = \left.\frac{\partial C_L}{\partial T}\right|_{z=int}\left.\frac{\partial T}{\partial r}\right|_{z=int} \tag{6}$$

are assumed. These are the same assumption as the one-dimensional TLZ model[3], that is, the concentration in the liquid is a function of only the temperature. Thus, the equation of

$$(C_L - C_S)\frac{\partial f}{\partial t} = -D\frac{\partial C_L}{\partial T}\left(\frac{\partial T}{\partial z} - \frac{\partial T}{\partial r}\frac{\partial f}{\partial r}\right)_L \tag{7}$$

is obtained. This is the two-dimensional TLZ model. On the other hand, the one-dimensional TLZ model[3] is described as

$$(C_L - C_S)R = -D\frac{\partial C_L}{\partial T}\left.\frac{\partial T}{\partial z}\right|_L, \tag{8}$$

where R is a growth rate. By comparing Eq. (7) with Eq. (8), it is found that the term of $-\frac{\partial T}{\partial r}\frac{\partial f}{\partial r}$ changes the growth rate estimated from the one-dimensional model. This means that the following expression is used as the definition of the two-dimensionality δ;

$$\delta = \left.-\frac{\partial T}{\partial r}\frac{\partial f}{\partial r}\right/\frac{\partial T}{\partial z}. \tag{9}$$

Two-dimensional Numerical Simulation

In order to calculate Eq. (9), temperature gradients along r- and z-directions and an interface shape are required. To obtain these parameters, two-dimensional numerical simulations are carried out. In the simulation, the energy transport equation, the mass transport equation, the stream function equation, the vorticity transport equation, the energy balance equation and the mass balance equation are simultaneously solved. We use the boundary fitted

coordinate (BFC) method[4-11], which is a kind of finite difference method, in order to solve these equations. The BFC method solves the governing equations that are transformed from the physical space to the computational space. The transformed governing equations are described as Eqs. (10) − (16).

$$\rho C_p\left\{\frac{\partial T}{\partial t}-\frac{1}{J}(z_\eta T_\xi - z_\xi T_\eta)\frac{\partial r}{\partial t}-\frac{1}{J}(-r_\eta T_\xi + r_\xi T_\eta)\frac{\partial z}{\partial t}\right\}-\rho C_p\frac{1}{r}\frac{1}{J}(\psi_\xi T_\eta-\psi_\eta T_\xi), \tag{10}$$
$$=k\frac{1}{J^2}(\alpha T_{\xi\xi}-2\beta T_{\xi\eta}+\gamma T_{\eta\eta})+k\frac{1}{r}\frac{1}{J}(z_\eta T_\xi - z_\xi T_\eta)$$

$$\frac{\partial C_L}{\partial t}-\frac{1}{J}(z_\eta C_{L\xi}-z_\xi C_{L\eta})\frac{\partial r}{\partial t}-\frac{1}{J}(-r_\eta C_{L\xi}+r_\xi C_{L\eta})\frac{\partial z}{\partial t}-\frac{1}{r}\frac{1}{J}(\psi_\xi C_{L\eta}-\psi_\eta C_{L\xi}), \tag{11}$$
$$=D_L\frac{1}{J^2}(\alpha C_{L\xi\xi}-2\beta C_{L\xi\eta}+\gamma C_{L\eta\eta})+D_L\frac{1}{r}\frac{1}{J}(z_\eta C_{L\xi}-z_\xi C_{L\eta})$$

$$\frac{\partial C_S}{\partial t}-\frac{1}{J}(z_\eta C_{S\xi}-z_\xi C_{S\eta})\frac{\partial r}{\partial t}-\frac{1}{J}(-r_\eta C_{S\xi}+r_\xi C_{S\eta})\frac{\partial z}{\partial t}, \tag{12}$$
$$=D_S\frac{1}{J^2}(\alpha C_{S\xi\xi}-2\beta C_{S\xi\eta}+\gamma C_{S\eta\eta})+D_S\frac{1}{r}\frac{1}{J}(z_\eta C_{S\xi}-z_\xi C_{S\eta})$$

$$-rJ^2\omega$$
$$=\alpha\psi_{\xi\xi}-2\beta\psi_{\xi\eta}+\gamma\psi_{\eta\eta}, \tag{13}$$
$$-\frac{J}{r}(z_\eta\psi_\xi - z_\xi\psi_\eta)$$

$$\frac{\partial\omega}{\partial t}-\frac{1}{J}(z_\eta\omega_\xi - z_\xi\omega_\eta)\frac{\partial r}{\partial t}-\frac{1}{J}(r_\eta\omega_\xi - r_\xi\omega_\eta)\frac{\partial z}{\partial t}+\frac{1}{r}\frac{1}{J^2}(-r_\eta\psi_\xi+r_\xi\psi_\eta)\cdot(z_\eta\omega_\xi - z_\xi\omega_\eta)$$
$$-\frac{1}{r}\frac{1}{J^2}(z_\eta\psi_\xi - z_\xi\psi_\eta)\cdot(-r_\eta\omega_\xi+r_\xi\omega_\eta)-\frac{1}{r^2}\frac{1}{J}\omega(-r_\eta\psi_\xi+r_\xi\psi_\eta)$$
$$=\nu\frac{1}{J^2}(\alpha\omega_{\xi\xi}-2\beta\omega_{\xi\eta}+\gamma\omega_{\eta\eta})+\nu\frac{1}{r}\frac{1}{J}(z_\eta\omega_\xi - z_\xi\omega_\eta)-\nu\frac{1}{r^2}\omega$$
$$+\frac{1}{J}Bg(z_\eta T_\xi - z_\xi T_\eta)+\frac{1}{J}Gg(z_\eta C_\xi - z_\xi C_\eta), \tag{14}$$

$$L_{SL}\rho\frac{\partial f}{\partial t}$$
$$=-k_L\frac{1}{r_\xi}\frac{1}{J_L}(-\beta T_\xi+\gamma T_\eta)_L, \tag{15}$$
$$+k_S\frac{1}{r_\xi}\frac{1}{J_S}(-\beta T_\xi+\gamma T_\eta)_S$$

$$(C_L-C_S)\frac{\partial f}{\partial t},$$
$$=-D_L\frac{1}{r_\xi}\frac{1}{J_L}(-\beta C_{L\xi}+\gamma C_{L\eta})_L \tag{16}$$

where $\alpha = r_\eta^2 + z_\eta^2$, $\beta = r_\xi r_\eta + z_\xi z_\eta$, $\gamma = r_\xi^2 + z_\xi^2$, $J = r_\xi z_\eta - r_\eta z_\xi$, ξ and η are the computational coordinates corresponding to r and z in the physical space, ψ the stream function, ω vorticity, T temperature, ρ density, C_p specific heat, κ thermal conductivity, ν kinetic viscosity, L_{SL} latent heat, B thermal volume expansion coefficient, G the buoyancy coefficient by the specific gravity difference, g gravity, t time, C the concentration, D the diffusion coefficient. Subscripts of L and S indicate the liquid side and the solid side, respectively.

Results and Discussion

The typical results of the numerical simulation in the case of the sample diameter of 2 mm and 10 mm are shown in Fig. 1 and 2, respectively. The gravity condition is 1 g. The thermal convection in the 2 mm case is weaker than that in the 10 mm case due to both the small diameter and the radially small variation of the temperature. For example, the convection effect on the mass transport is negligibly small in the 2 mm case[12] due to the weak convection. In addition, the two-dimensionality may be also negligibly small in the 2 mm case. By using the numerical results, the two-dimensionality is calculated and is shown in Fig. 3 as a function of the radius. In this figure, the two-dimensionality in the 2 mm, 5 mm and 10 mm cases are plotted as the red line, the blue line and the green line, respectively. As shown in Fig. 3, the two-dimensionality in the 2 mm case is only about 4 % at the maximum. This result indicates that the radial difference of the growth rate in the 2 mm case is within ± 0.01 mm/hr since the growth rate is about 0.216 mm/hr in the ground-based crystal growth experiments. The difference of ± 0.01 mm/hr is usually negligibly small from the viewpoint of the experimental technique. However, the two-dimensionality increases with the sample diameter, that is, about 16 % in the 5 mm case and about 33 % in the 10 mm case at the maximum. These values are not negligible and this should be one of the reasons that a homogeneous crystal growth with a large diameter is difficult on the ground. The two-dimensionality increases as the radial position increases as a macroscopic tendency. This tendency indicates that the InAs mole fraction in the solid decreases as the crystal grows near the outer radius if the InAs fraction is almost constant on the axis. This is qualitatively consistent with the experimentally obtained InAs mole fraction in the 10 mm case as shown in Fig. 4. Although the data scattering in Fig. 4 may be caused by grain boundaries, the mole fraction variation can be clearly observed.

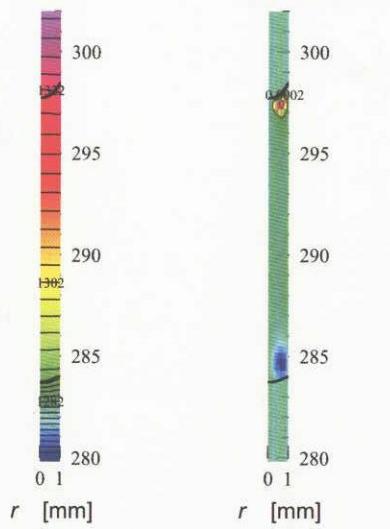

(a) Temperature (b) Stream Function

Fig. 1 Typical results in 2 mm case

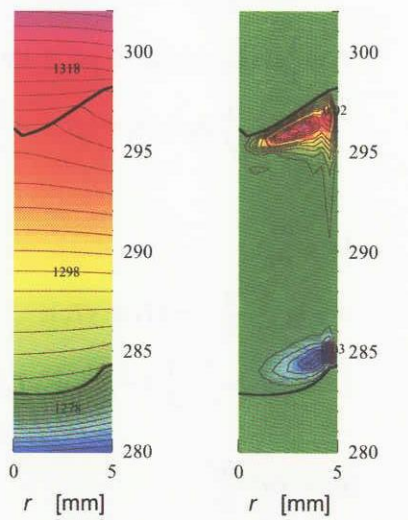

(a) Temperature (b) Stream Function

Fig. 2 Typical results in 10 mm case

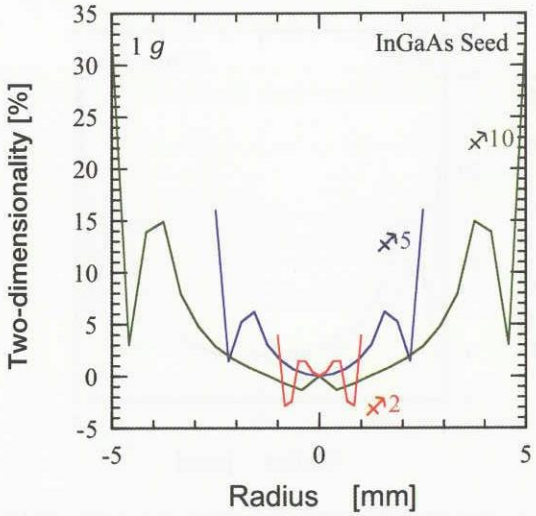

Fig. 3 Radial variation of two-dimensionality

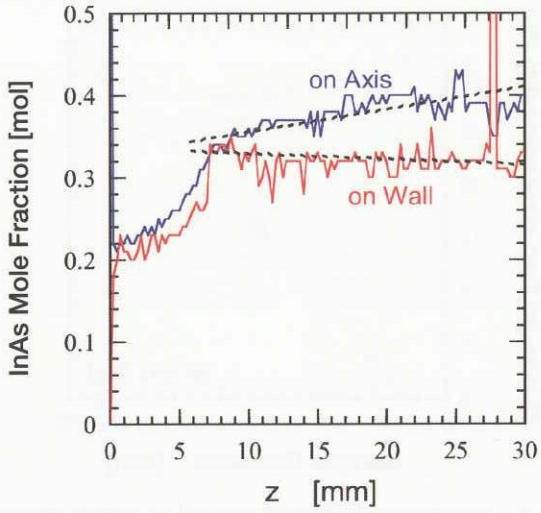

Fig. 4 Experimentally obtained InAs mole fraction along growth direction

As shown in Fig. 3, the two-dimensionality once decreases near the crucible wall then is maximized on the wall. This means that the lattice mismatch is maximized near the wall. This may enhance polycrystallization. The combination of this lattice mismatch with the constitutional supercooling on the wall may be the reason that single crystal growth is difficult on the ground. This issue should be investigated more deeply in future. By plotting the maximum two-dimensionality, the dependency of the two-dimensionality on the sample diameter is obtained and is shown in Fig. 5. By fitting the second order curve, the sample diameter, at which the two-dimensionality is zero, is estimated and is slightly larger than 1 mm. This estimation indicates that the two-dimensionality becomes almost perfectly negligible if the sample diameter is 1 mm.

The thermal convection may enhance the two-dimensionality. Therefore, the two-dimensionality variation against the gravity condition is investigated. Figure 6 is the comparison between the two-dimensionality under 1 g condition and that under no gravity condition. The red line and the blue one represent the two-dimensionality under 0 g and that under 1 g. This figure shows that the two-dimensionality under 0 g is smaller than that under 1 g. However, the two-dimensionality under 0 g is about 26 %, while the two-dimensionality under 1 g is about 33 %. This is not small enough to obtain a homogeneous crystal. This result indicates that the contribution of the convection to the two-dimensionality is not so large. Another possibility of the large two-dimensionality is the thermal conductivity difference between the seed crystal and the crucible. Namely, the heat is mainly transferred to the wall at the interface rather than to the seed crystal. If this speculation is true, the two-dimensionality should decrease by using another seed, of which the thermal conductivity is higher than that of the InGaAs crystal, for example, a GaAs seed. The thermal conductivity of the GaAs is about 16.0 W/K·m, while that of the $In_{0.3}Ga_{0.7}As$ is about 3.0 W/K·m. The effect of the GaAs seed on the two-dimensionality is investigated. The result is shown in Fig. 7. This figure clearly shows that the two-dimensionality in the GaAs seed case is drastically small as compared with that in the InGaAs seed case. It is summarized that the GaAs seed is much appropriate for the homogeneous crystal growth with a large diameter from the viewpoint of the two-dimensionality. However, the lattice mismatch at the initial interface may prevent single crystal growth. So this issue should also need further investigation in future.

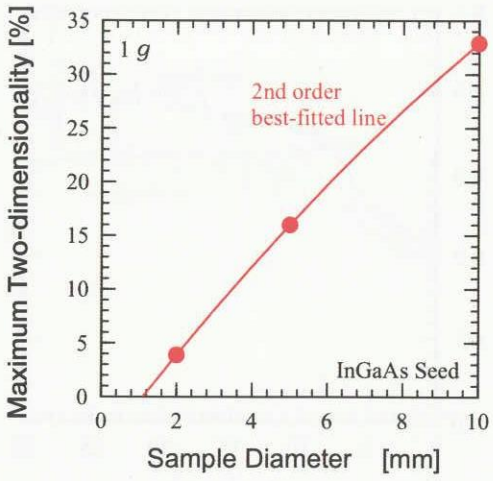

Fig. 5 Two-dimensionality dependency on sample diameter

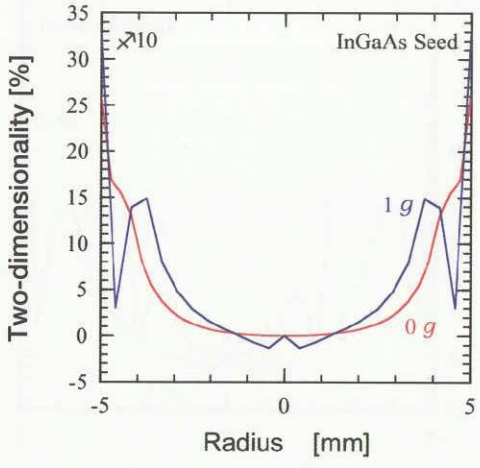

Fig. 6 Two-dimensionality comparison in 1 g case and in 0 g case

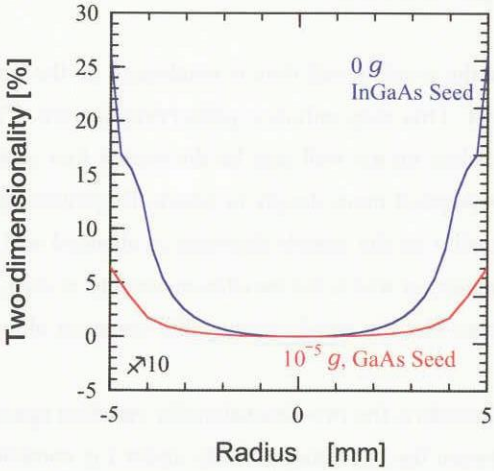

Fig. 7 Two-dimensionality variation in InGaAs seed case and in GaAs seed case

Conclusions

By introducing a new two-dimensional TLZ model, the two-dimensionality is defined from the viewpoint of the interface shape. To calculate the two-dimensionality, two-dimensional numerical simulations are carried out. By using the numerical results, the two-dimensionality is calculated in various sample diameters. In the case of the sample diameter of 2 mm, the two-dimensionality is about 4 % at maximum on the ground. This is small enough to grow a homogeneous crystal. On the other hand, in both the 5 mm and the 10 mm cases, the two-dimensionality is about 16 % and 33 % at the maximum, respectively. These values are not negligible and this may be one of the reasons why homogeneous crystal growth with a large diameter is difficult on the ground. Because the thermal convection becomes strong as the sample diameter increases, the increases of the two-dimensionality in the 5 mm and the 10 mm cases may be caused by the convection. Therefore the two-dimensionality under the 0 g condition is investigated. From the comparison of the two-dimensionality in 1 g with that in 0 g, the decrease of the two-dimensionality is not enough though it decreases under the 0 g condition. This suggests that the large two-dimensionality is caused

another mechanism rather than the convection. To investigate this speculation, the two-dimensionality in the GaAs seed case is calculated. From the result, it is found that the two-dimensionality is drastically reduced. Therefore, the GaAs seed is much appropriate for homogeneous crystal growth. However, the lattice mismatch at the initial interface may cause polycrystallization. This issue will be investigated in future.

References

[1] K. Kinoshita, H. Kato, M. Iwai, T. Tsuru, Y. Muramatsu, S. Yoda : J. Cryst. Growth 225 (2001) 59-66.

[2] K. Kinoshita, Y. Hanaue, H. Nakamura, S. Yoda, M. Iwai, T. Tsuru, Y. Muramatsu : J. Cryst. Growth 237-239 (2002) 1859-1863.

[3] H. Nakamura, Y. Hanaue, H. Kato, K. Kinoshita S. Yoda, J. Cryst. Growth 258 (2003) 49.

[4] J. F. Thompson, F. C. Thames and C. W. Mastin : J. Comp. Phys. 15 (1974) 299.

[5] K. Fujii : Numerical *Methods for Computational Fluid* Dynamics (Tokyo Univ., Tokyo, 1994) 2nd ed., Chap. 7 [in Japanese].

[6] H. Takami and T. Kawamura: *Numerical Solution of Partial Differential Equations by the Finite Difference Method* (Tokyo Univ., Tokyo, 1994) 2nd ed., Chap. 6 [in Japanese].

[7] M. Saitou: Inst. Electron. Mater. Tech. Note 7 (1989) No. 2, 15 [in Japanese].

[8] J. S. Szmyd and K. Suzuki (Ed.) : *Modeling of Transport Phenomena in Crystal Growth* (WIT Press, Southampton, 2000), Chap. 4.

[9] S. Adachi, K. Kawachi, M. Kaneko, H. Kato, S. Yoda and K. Kinoshita : *Reliability Investigation on Numerical Analysis by Comparison with Experimental Result* (Annual Report of the Semiconductor Team in NASDA Space Utilization Research Program, 2000).

[10] S. Adachi, S. Yoda, and K. Kinoshita : *Numerical Analysis of a Cartridge in the Traveling Liquidus-Zone Method under Various Gravity Conditions* (Annual Report of the Semiconductor Team in NASDA Space Utilization Research Program, 2001).

[11] S. Adachi, N. Koshikawa, S. Matsumoto, S. Yoda, and K. Kinoshita : *Numerical Investigation on Two-dimensionality in a Flight Cartridge* (Annual Report of the Semiconductor Team in NASDA Space Utilization Research Program, 2003).

[12] S. Adachi, Y. Ogata, N. Koshikawa, S. Matsumoto, K. Kinoshita, M. Takayanagi, S. Yoda: J. Cryst. Growth 267 (2004) 417.